TYPE Mini Review
PUBLISHED 27 June 2023
DOI 10.3389/fphot.2023.1213434

OPEN ACCESS

EDITED BY
Michele Ortolani,
Sapienza University of Rome, Italy

REVIEWED BY
Tommaso Giovannini,
Scuola Normale Superiore, Italy

*CORRESPONDENCE
B. Hinkov,
borislav.hinkov@tuwien.ac.at

RECEIVED 27 April 2023
ACCEPTED 08 June 2023
PUBLISHED 27 June 2023

CITATION
Hinkov B, David M, Strasser G, Schwarz B and Lendl B (2023), On-chip liquid sensing using mid-IR plasmonics.
Front. Photonics 4:1213434.
doi: 10.3389/fphot.2023.1213434

On-chip liquid sensing using mid-IR plasmonics

B. Hinkov[1]*, M. David[1], G. Strasser[1], B. Schwarz[1] and B. Lendl[2]

[1]Institute of Solid State Electronics and Center for Micro- and Nanostructures, Technische Universität (TU) Wien, Vienna, Austria, [2]Institute of Chemical Technologies and Analytics, Technische Universität (TU) Wien, Vienna, Austria

The investigation of molecules in the mid-IR spectral range has revolutionized our understanding in many fields such as atmospheric chemistry and environmental sensing for climate research or disease monitoring in medical diagnosis. While the mid-IR analysis of gas-samples is already a mature discipline, the spectroscopy of liquids is still in its infancy. However, it is a rapidly developing field of research, set to fundamentally change our knowledge of dynamical processes of molecules in liquid-phase. In this field, mid-IR plasmonics has emerged as breakthrough concept for miniaturization, enabling highly-sensitive and -selective liquid measurement tools. In this review, we give an overview over current trends and recent developments in the field of mid-IR spectroscopy of molecules in liquid phase. Special attention is given to plasmon-enhanced concepts that allow measurements in highly compact sensor schemes. Nowadays, they reach full monolithic integration, including laser, interaction section and detector on the same chip, demonstrating unprecedented operation in *situ* and real-time analysis of chemical processes.

KEYWORDS

mid-infrared plasmonics, lab-on-a-chip, liquid sensing, bio-sensing, proteins, *in situ*, quantum cascade laser, optoelectronics

1 Introduction

Semiconductors have transformed our everyday life in a variety of different ways (Bardeen and Brattain, 1948; Hall et al., 1962; Huang et al., 2020; Fraunhofer-ISE, 2022; Huang et al., 2022). They are known to be fundamental components of computers and mobile phones, but nowadays also enter in other fields when being implemented into fridges and baking ovens as remotely controllable parts in the "internet of things." In particular, semiconductor-based optoelectronics is a field of compact devices for the conversion of electrical into optical signals like in LEDs (Cho et al., 2017; Huang et al., 2020) and (diode) lasers (Hall et al., 1962; Faist et al., 1994; Yang, 1995), or *vice versa*, for generating electrical signals from measuring photons in detectors and imaging instruments (Broudy and Mazurczyk, 1981; Levine et al., 1987; Hofstetter et al., 2002; Yang et al., 2010). While for decades optoelectronic devices have already been the backbone of our data transmission and telecommunication infrastructure (Nadiri and Nandi, 2003; Dely et al., 2022; Flannigan et al., 2022; Pang et al., 2022; Submarine Communication, 2023), they are becoming increasingly relevant in molecular spectroscopy in recent years (Curl et al., 2010; Celebrano et al., 2011; Haas and Mizaikoff, 2016; Hinkov et al., 2022).

2 Light sources in the mid-IR spectral range

The mid-IR spectral range is the part of the electromagnetic spectrum, hosting the fundamental vibrational "fingerprint" absorptions of many molecules (Li et al., 2013; Schwaighofer and Lendl, 2020; CFA, 2023). For their detection, they are typically analyzed using thermal- or laser-based light sources. The former often use globars (Yashunsky et al., 2010; Haas and Mizaikoff, 2016) (a SiC-rod heated to ~1,250°C) in Fourier-transform infrared (FTIR-)spectrometers, being able to obtain full mid-IR spectra from 400 to 4,000 cm^{-1} in a single-shot measurement on the seconds-to-few-minutes time-scale (Baker et al., 2014; Baumgartner et al., 2018; De Meutter and Goormaghtigh, 2021; Schwaighofer et al., 2021; Szwarcman et al., 2021). However, their major drawback is a very low emission power per wavelength in the $\mu W/cm^{-1}$ range (Brandstetter et al., 2010; Schwaighofer and Lendl, 2020), which is a particular issue in liquids. On the contrary, the probably most widely used mid-IR lasers are the quantum cascade laser (QCL) that was first demonstrated by Faist et al. (1994) and the interband cascade laser (ICL) that was realized for the first time by Yang et al., in 1995 (Yang, 1995). QCLs exploit tailored intersubband transitions in quantum wells, allowing to design their emission wavelength by bandstructure engineering (Faist, 2013) from ~3–12 μm (Bai et al., 2011; Lyakh et al., 2012a; Bismuto et al., 2012; Hinkov et al., 2013; Schwarz et al., 2017). In contrast, ICLs use a type-II band alignment active region based on tailorable interband transitions and show strong performance in the range of ~2.8–6 μm wavelength (Vurgaftman et al., 2013; Scheuermann et al., 2015). Today, both, QCLs and ICLs, are highly-reliable and versatile mid-IR laser light sources with room-temperature (RT) and continuous-wave (CW) operation (Bai et al., 2011; Lyakh et al., 2012b; Hinkov et al., 2012; Vurgaftman et al., 2013; Weih et al., 2014; Schwarz et al., 2017; Knötig et al., 2020; Meyer et al., 2020). State-of-the-art devices emit up to ~6-9 orders of magnitude higher spectral power densities (= $W\text{-}kW/cm^{-1}$) (Vurgaftman et al., 2013; Schwaighofer and Lendl, 2020) than globars, and they can be further scaled up by using very narrow linewidth singlemode devices based on distributed feedback (DFB) gratings (Bartalini et al., 2011; Tombez et al., 2012). The much narrower spectral coverage of mid-IR laser emission as compared to globars can be significantly increased by using widely tunable external-cavity (EC) lasers (Wysocki et al., 2005; Hinkov et al., 2009; Hugi et al., 2009; Fuchs et al., 2010; Riedi et al., 2013), DFB devices (Faist et al., 1997; Lu et al., 2011; Xie et al., 2012; Suess et al., 2016; Hinkov et al., 2019) extended to multi-wavelengths array geometries (Mujagić et al., 2011; Rauter et al., 2013; Jouy et al., 2015; Süess et al., 2016; Marschick et al., 2023) or frequency comb configurations (Villares et al., 2014; Consolino et al., 2020; Sterczewski et al., 2020; Komagata et al., 2023). One important additional feature of those mid-IR lasers relevant for miniaturization towards chip-scale applications, is their ability to be used as QC detectors (QCDs) (Hofstetter et al., 2002) or IC infrared photodetectors (ICIPs) (Li et al., 2005; Yang et al., 2010), respectively. QCDs are typically operated unbiased (Hofstetter et al., 2002; Reininger et al., 2013; Delga, 2020; Marschick et al., 2022), show low dark current detection (Delga, 2020; Marschick et al., 2022), similar to QCLs, GHz-bandwidth operation (Hinkov et al., 2016; Dely et al., 2022) and a large range of linear response, even at high power levels (Dabrowska et al., 2022; Marschick et al., 2022). It is important to note, that QC devices are ideal candidates for integration with plasmonic concepts, since they inherently support TM-polarization only (Faist, 2013; Jollivet et al., 2018; Delga, 2020). This enables direct excitation of surface plasmon polaritons (SPPs) in suitable surface geometries.

3 Mid-IR spectroscopy

The mid-IR spectral range hosts many important applications such as sensing of environmental greenhouse gases (Kosterev et al., 2008; Tuzson et al., 2008; EPA, 2014; IPCC, 2022), pharmaceutical analysis and production techniques as well as petrochemical applications (ASTM D6304 – 16, 2021; Garcia-Perez et al., 2008; Ricchiuti et al., 2022; Pilat et al., 2023), point-of-care medical diagnosis including *in situ* bio-medical analysis and wearables (Pleitez Rafael et al., 2013; Baldassarre et al., 2016; Lu et al., 2020; Smuck et al., 2021), spectral imaging (Amrania et al., 2018; Kilgus et al., 2018; Razeghi, 2020) and security applications (Pushkarsky et al., 2006; Fuchs et al., 2010; Hinkov et al., 2010). In addition, it is rapidly unlocked for optical free-space communication with Gbit s^{-1} transmission rates (Dely et al., 2022; Flannigan et al., 2022; Pang et al., 2022) in the spectral windows of low atmospheric attenuation between 3–5 μm and 8–12 μm wavelength (Flannigan et al., 2022; CFA, 2023). Mid-IR spectroscopy analyzes molecules in gas (Curl et al., 2010; Patimisco et al., 2014; Haas and Mizaikoff, 2016; Schwaighofer et al., 2017; Szedlak et al., 2018; Hinkov et al., 2019; Waclawek et al., 2019), liquid (Murayama and Tomida, 2004; Barth, 2007; Barreca et al., 2010; De La Arada et al., 2012; Amenabar et al., 2013; Mizaikoff, 2013; Pleitez Rafael et al., 2013; Lu et al., 2015; Rodrigo et al., 2015; Güler et al., 2016; Schwaighofer et al., 2016; Bibikova et al., 2017; Barelli et al., 2020; Chowdhury et al., 2020; Norahan et al., 2021; Szwarcman et al., 2021) and solid phase (Fuchs et al., 2010; Hinkov et al., 2010; Celebrano et al., 2011; Amrania et al., 2012; Amrania et al., 2018). Gas-sensing is probably the most developed field among them, addressing the very narrow absorption lines of gas-molecules (< 1 cm^{-1}) (Li et al., 2013; Tuzson et al., 2013; CFA, 2023). This finds application in many fields including isotope spectroscopy (Kerstel, 2003; Bartlome and Sigrist, 2009; Li et al., 2013; Wunderlin et al., 2013) of CO_2 (Tuzson et al., 2013; Van Geldern et al., 2014; Wang et al., 2017) for emission source identification based on monitoring isotope-resolved concentration patterns. In the past 2 decades, numerous high-sensitivity and -selectivity gas-sensing techniques have been developed, based on direct absorption spectroscopy following the Beer-Lambert absorption law (Barth, 2007; Tuzson et al., 2013). Due to the large absorption length (distance into the medium for 1/*e*-signal-attenuation) when measuring in gases, they often rely on increasing the effective path length in the gas analyte up to the meter-scale, e.g., by multi-reflection gas cells which simultaneously also decrease the sensor footprint (Li et al., 2013; Tuzson et al., 2013). Instead, alternative advanced spectroscopic schemes measure other quantities and thus can implement specific capabilities. Prominent examples are: i) the baseline-free chirped laser dispersion spectroscopy (CLaDS), probing the refractive index change in a gas, ii) (quartz-enhanced) photoacoustic spectroscopy (QEPAS) (Kosterev et al., 2008; Patimisco et al., 2018; Ma et al.,

2022) that analyzes a generated periodic acoustic wave with a (quartz-)tuning fork and can be calibration-free (Wu et al., 2017), iii) balanced interferometric cavity assisted photothermal spectroscopy (B-ICAPS) (Waclawek et al., 2016; Waclawek et al., 2019), which again probes refractive index changes, but this time through a generated photothermal signal, and which scales linearly with gas concentration and is suitable for sensor miniaturization (Waclawek et al., 2016) and iv) dual-comb spectroscopy with mid-IR QCL (Villares et al., 2014; Consolino et al., 2020; Komagata et al., 2023) or ICL frequency combs (Sterczewski et al., 2020), which relies on analyzing a heterodyne beating signal. In contrast to gas-phase spectroscopy, detecting molecules in liquid-phase needs to address broad absorption features ($\gg$50 cm^{-1}) in a much denser medium (Schwaighofer and Lendl, 2020). While the former demands for broadband sensors, the latter results in orders of magnitude lower absorption lengths. Typical corresponding penetration lengths in highly absorbing aqueous solutions are a few micrometers only for thermal-light-source-based sensors like FTIR-spectrometers (Fabian and Mäntele, 2006; Haas and Mizaikoff, 2016; Schwaighofer and Lendl, 2020; Dabrowska et al., 2022) and can reach up to tens of micrometers (Schwaighofer et al., 2016; Akhgar et al., 2020; Schwaighofer et al., 2021) and above (Schwarz et al., 2014; Hinkov et al., 2022) for laser-based techniques. It can be further significantly increased by using a low-absorbing matrix, e.g., D_2O instead of H_2O for protein analysis in the amide I band (Murayama and Tomida, 2004; Barreca et al., 2010; De La Arada et al., 2012; Lu et al., 2015; Yang et al., 2015; Güler et al., 2016; Strazdaite et al., 2020; De Meutter and Goormaghtigh, 2021).

4 Protein-sensing with discrete optical components

While FTIR-based liquid sensing approaches are currently getting more and more substituted or complemented by laser-based techniques, state-of-the-art measurement and analysis tools are still often using tabletop geometries with discrete components. Protein-sensing in the mid-IR is a field of research of high relevance for pharmaceutical and bio-medical applications (Baldassarre et al., 2016; Schwaighofer et al., 2017; Kumar et al., 2018; Shrivastav et al., 2021; Altug et al., 2022) with a rich body of existing literature (Barth, 2007; Baldassarre et al., 2016; López-Lorente et al., 2017; Kumar et al., 2018; Shrivastav et al., 2021; Szwarcman et al., 2021; Altug et al., 2022). It will act as prototype-field in this review paper for discussing typical discrete-component measurement systems, including for the analysis of e. g., poly-l-lysine (PLL) (Schwaighofer and Lendl, 2020; Mousavi et al., 2021), bovine serum albumin (BSA) (Murayama and Tomida, 2004; Barreca et al., 2010; Lu et al., 2015; Güler et al., 2016; Schwaighofer et al., 2016; De Meutter and Goormaghtigh, 2021; Hinkov et al., 2022), α-Chymotrypsin (Yang et al., 2015) or the milk proteins β-lactoglobulin, α-lactalbumin and casein (Dabrowska et al., 2022). Those proteins are traditionally analyzed in the "protein fingerprint region", the amide I band between 1,600–1700 cm^{-1}, which mainly arises from their C=O stretching vibration with some other minor contributions (Barth and Zscherp, 2002). Measuring proteins in the mid-IR enables access to their structural properties, such as the protein secondary structure, which are essential for protein function (Murayama and Tomida, 2004; Lu et al., 2015; Yang et al., 2015; Güler et al., 2016; Schwaighofer et al., 2016; De Meutter and Goormaghtigh, 2021; Hinkov et al., 2022). Those properties were recently exploited by Schwaighofer et al. (2016), who analyzed the thermal denaturation of the secondary structure of the polypeptide PLL in the amide I range with an EC-QCL, a Mercury cadmium telluride (MCT-)detector and a temperature-controlled flow cell. Using deuterated solution allowed a film thickness of 478 μm for monitoring concentrations of 0.25–10 mg mL^{-1} under controlled pH-conditions. Lu et al. (Lu et al., 2015) investigated the thermal denaturation of BSA in D_2O buffer, identifying two different temperature ranges (50°C–52°C and 80°C–82°C) for protein structure changes. They used a FTIR-MCT setup and a flow cell equipped with an ATR-based silver-halide fiber sensor for 290 μm films. Yang et al. (Yang et al., 2015) published a FTIR-based routine for analyzing the protein secondary structure of e.g., α-Chymotrypsin and other proteins at high concentrations above 3 mg mL^{-1} in aqueous solution (H_2O and D_2O). And Dabrowska et al. (Dabrowska et al., 2022) analyze the bovine milk proteins β-lactoglobulin, α-lactalbumin and casein in a broadband EC-QCL-QCD setup covering a spectral range above 260 cm^{-1} for concentrations of 0.25–15 mg mL^{-1} and a film thickness of 12.5 μm. Multivariate sample analysis of protein mixtures using the partial least square (PLS) method, allows identifying individual constituents at high figures-of-merit (R^2 > 0.98).

5 Compact liquid sensing schemes based on mid-IR plasmonics

While FTIR- and laser-based techniques have revolutionized the field of mid-IR liquid sensing, their often rather bulky experimental geometries do not allow sensing on rapid time-scales or even *in situ* sample analysis. A wide range of novel and suitable approaches targets this issue by miniaturized mid-IR sensors based on the exploitation of plasmonic concepts (Homola, 2006; Biagioni et al., 2012; Rodrigo et al., 2015; Neubrech et al., 2017; Taliercio and Biagioni, 2019; Barelli et al., 2020; Altug et al., 2022; Hinkov et al., 2022). SPPs are collective oscillations of the electron density at the intersection of two materials with sign change of the real part of their electrical permittivity, such as at a metal-dielectric interface (Sarid, 1981). From their dispersion relation, the condition for the permittivity ϵ of both materials for successful SPP excitation and propagation can be derived to be: $|\epsilon_m| > \epsilon_d$ (m: metal and d: dielectric permittivity) (Law et al., 2013). Corresponding, highly confined sub-wavelength plasmonic modes (Barnes et al., 2003; Ozbay, 2006; Falk et al., 2009) enable high-speed photonic properties and below-diffraction-limit device miniaturization for visible (Guo et al., 2013; Huang and Luo, 2018; Sistani et al., 2019) to near-IR wavelengths (Huang and Luo, 2018; Sistani et al., 2019), with electrical wire (Falk et al., 2009; Guo et al., 2013) to optical waveguide geometries (Ozbay, 2006; Lal et al., 2007; Guo et al., 2013; David et al., 2021). While strong confinement to a metallic surface yields high guiding losses and limited propagation lengths (Guo et al., 2013), still high-performance and high-speed SPP as well as localized surface plasmon (LSP) detectors can be realized (Huang and Luo, 2018; Sistani et al., 2019; Sistani et al., 2020). LSPs are the localized counterpart of SPPs, typically excited in metallic nanostructures (Law et al., 2013; Bibikova et al., 2017; López-Lorente et al., 2017).

5.1 Recent developments in mid-IR plasmonics

The above described SPP and LSP concepts work very well for UV to near-IR wavelengths based on the use of (noble or transition) metals (Au, Ag, Ni, Cu (Aroca et al., 2004; Law et al., 2013; Perry et al., 2013)) with their plasma-frequencies in the deep-UV to visible range. The situation is completely different in the mid-IR spectral range. The permittivity $|\epsilon_m|$ is much larger (also than ϵ_d), yielding a much higher plasmonic mode extension into the dielectric, e.g., ~3x to >10x the modal wavelength for an Ag/air interface (Law et al., 2013). This results in a significantly larger mode propagation length on the order of above 1,000x wavelengths (mm-scale) (Law et al., 2013). Unfortunately, it is not always useful for mid-IR liquid-sensing applications, where coupling to active or passive on-chip components on the wavelength-scale is needed. For avoiding those limitations of metal-based mid-IR plasmonics, lower-plasma-frequency materials have been demonstrated, including highly-doped epitaxial semiconductors (Taliercio and Biagioni, 2019; Ehlers and Mills, 1987; Gómez Rivas et al., 2004; Ginn et al., 2011; Law et al., 2012; N'tsame Guilengui et al., 2012; Augel et al., 2016; Frigerio et al., 2016; Pellegrini et al., 2018), such as Ge, Si, III-Vs (e.g., GaP and GaN) or II-VIs (Barker, 1968; Harima et al., 1998; Streyer et al., 2014; Zhong et al., 2015; Taliercio and Biagioni, 2019), transparent conductive oxides (Zhong et al., 2015; Castellano, 2022), silicides (Soref et al., 2008; Naik et al., 2013; Zhong et al., 2015), transition metal nitrides (Zhong et al., 2015) and graphene (Fei et al., 2012; Grigorenko et al., 2012; Zhong et al., 2015; Constant et al., 2016). However, they mainly fit to Si-photonics integration or to implementation into CMOS-structures and lack simple fabrication and implementation protocols, compatible with mid-IR technology. As an alternative approach, structured-metal "spoof" SPP geometries are an interesting option (Pendry et al., 2004; Williams et al., 2008; Yu et al., 2008) that has been used to pattern QCL-facets to collimate their output beam in mid-IR (Yu et al., 2008) or THz devices (Yu et al., 2010). Lately, the concept of combining dielectric loading (DL) with noble metal plasmonics is generating significant interest. It has previously been used at telecom wavelengths (Holmgaard and Bozhevolnyi, 2007; Steinberger et al., 2007; Kumar et al., 2013; Krasavin and Zayats, 2015) and shows similarities to hybrid plasmonic concepts (Nielsen et al., 2014; Zhang et al., 2017). At near-IR wavelengths, DLSPP waveguides have been used because of their: i) direct control over the trade-off between mode confinement and propagation length enabling complex plasmonic circuits and ii) their flexibility to use dielectric materials with particular thermo- or electro-optic properties (Kumar et al., 2013). In the mid-IR, DLSSP waveguides increase the vertical mode confinement significantly, allowing the realization of complex mid-IR photonic integrated circuits (PICs). By simply adding a ~200–300 nm thick slab of SiN (Schwarz et al., 2014) or Ge (David et al., 2021) to a ~100–200 nm thick Au layer for ~6.5–9.5 μm wavelength, the resulting SPP mode becomes vertically confined to the wavelength-scale, while maintaining up-to mm-scale propagation lengths (Schwarz et al., 2014; David et al., 2021). Since SiN absorbs above 7 μm (Kischkat et al., 2012), Ge can be a suitable alternative that is transparent in the whole mid-IR between 2 μm and 14 μm and that can be used in a similar way as dielectrics in DLSPPs, in so-called semiconductor loaded SPP (SLSPP) waveguides (David et al., 2021).

5.2 Plasmonic sensing concepts in the mid-IR

Highly-sensitive and -selective liquid-phase spectroscopy using compact metal-dielectric structures has been a well-established field for near-UV to near-IR wavelengths (Sreekanth et al., 2016). It enables overcoming diffraction limitations of conventional chip-scale approaches (Amenabar et al., 2013; Kilgus et al., 2018). For momentum mismatch compensation when coupling an external light source to such a SPP surface, mode coupling (Raether, 1988; Barnes et al., 2003) and control mechanisms (Raether, 1988; Yu et al., 2010; Thongrattanasiri et al., 2011) were introduced, by using external prisms (Otto or Kretschmann configuration) (Sreekanth et al., 2016; Castellano, 2022), by implementing high-index layers (Law et al., 2013) or by spoof SPP geometries (Pendry et al., 2004; Yu et al., 2010; Kushiyama et al., 2012; Law et al., 2013). In contrast, LSPs do not need momentum matching because of their tunability of the resonance frequency (Sreekanth et al., 2016) through altering the plasmonic particle shape or by modifying its dielectric environment (Law et al., 2013; Bibikova et al., 2017; López-Lorente et al., 2017). In the mid-IR, LSPs cannot be directly excited in sub-wavelength spheres and particles, which act as close to perfect conductors in this wavelength range ($|\epsilon_m| \to \infty$) and do not support plasmonic mode penetration into and coupling to their metallic surface. Again, materials with lower plasma frequency can be used (Taliercio and Biagioni, 2019; Ginn et al., 2011; Law et al., 2012; N'tsame Guilengui et al., 2012; Augel et al., 2016; Frigerio et al., 2016; Pellegrini et al., 2018; Zhong et al., 2015). Figure 1 shows a selection of metal-based mid-IR liquid sensor concepts, which are mainly relying on plasmonic enhancement (Figures 1B–D). Infrared reflection absorption spectroscopy (IRAS) (Figure 1A) is an early approach using molecules on homogeneous metal films and the only displayed non-plasmonic technique (Hoffman, 1983). Surface-enhanced IR absorption spectroscopy (SEIRA) (Figure 1B) (Osawa, 1997; Aroca et al., 2004) is probably the most widely used plasmonic sensing technique, where the light is coupled to LSPs on metal islands or nanostructures (Law et al., 2013). SEIRA supports local near-field molecular absorption enhancement with broadband spectral resonances, enabled by the random metal roughness of the surface islands. It was first demonstrated in 1980 by Hartstein et al. (1980) in silver nanoparticles and shares similarities with surface-enhanced Raman spectroscopy (SERS) (Fleischmann et al., 1974; Nie and Emory, 1997; Langer et al., 2020). It includes comparable signal values, even though both techniques show very different absorption enhancements of 10–1,000 (SEIRA) and 10^{14}-10^{15} (SERS) (Nie and Emory, 1997). SERS is beneficial for localized short-range molecule analysis, while SEIRA has advantages in probing thicker films. Prism-coupled SEIRA (Kretschmann or Otto configuration) (Figure 1C) combines localized field enhancement with SPP characteristics in patterned metal films (Hatta et al., 1984). It has also been used exploiting strong SPP enhancement in biological applications (Golosovsky et al., 2009). Finally, surface-plasmon-enhanced infrared absorption (SPEIRA) (Figure 1D) relies on exploiting the effect of extraordinary optical transmission (EOT) in metallic grating structures, e.g., in Au, Ag, Cu, Ni (Ebbesen et al., 1998; Martín-Moreno et al., 2001; Williams and Coe,

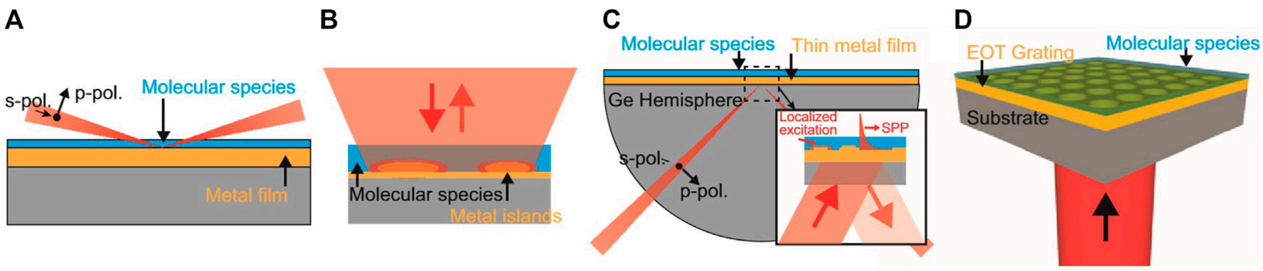

FIGURE 1
Schematics of various plasmonic sensing techniques: **(A)** IRAS. **(B)** Reflection-geometry SEIRA. **(C)** Kretschmann-configuration SEIRA for coupling through an external prism. **(D)** SPEIRA. Figure reprinted from Law et al. (2013), licensed under CC BY 3.0 with permission from the authors.

2006; Wasserman et al., 2007; Liu and Lalanne, 2008). Its enhancement factor is about x100 as compared to IRAS, resulting from a longer SPP-path length. Based on these plasmonic concepts, different compact liquid sensors have been realized. One often used geometry is based on attenuated total reflection (ATR) in surface-coated semiconductor crystals (e.g., Si or Ge) (Bibikova et al., 2017; López-Lorente et al., 2017; Wacht et al., 2022). In the work by Bibikova et al. (2017) and López-Lorente et al. (2017) nanoparticle-based resonant enhancement on top of Si-ATR-crystals was achieved by either using spherical gold nanoparticles and anisotropic gold nanostars for measuring thioglycolic acid (enhancement: 10x) or BSA (enhancement: 2x) in H_20 (Bibikova et al., 2017) or by using Au nanoparticles with BSA (enhancement: 2x) in H_20 and D_20 (López-Lorente et al., 2017). Another complementary SEIRA approach by Yoo et al. (2018) exploits a wafer scale array of zeroth-FP-order resonant coaxial nanoapertures with 7 nm gap size which analyzes 5 nm thick silk protein films. The result is an impressive absorption enhancement factor of 10^4–10^5. Additional work on SEIRA spectroscopy is summarized in the following two review papers: (Neubrech et al., 2017; Shrivastav et al., 2021). Neubrech et al. (2017) review the field of "resonant SEIRA", i.e., resonant metal nanoantennas including their underlying physics and routes for maximizing SEIRA enhancement based on the used geometry, arrangement and material. For more work on mid-IR plasmonic nanoantennas we refer to (Biagioni et al., 2012; Baldassarre et al., 2015; Celebrano et al., 2015; Celebrano et al., 2021; Di Francescantonio et al., 2022). The review by Shrivastav et al. (2021) gives an overview over current plasmonic-based biosensors for viral diagnostics based on SEIRA, propagating/localized surface-plasmon resonance (SPR) and SERS. Returning to plasmonic sensor concepts based on ATR geometries, Baumgartner et al. (Baumgartner et al., 2018; Baumgartner et al., 2019), Wacht et al. (2022) and Frank et al. (2021) show the functionalization of ATR-crystals for significantly enhanced sensitivity, by using Silica- (Baumgartner et al., 2018; Baumgartner et al., 2019), Zirconia- (Wacht et al., 2022) and Titania-based (Frank et al., 2021) ordered mesoporous films, respectively. Typically achieved enrichment factors lie on the order of >200 (benzonitrile, silica film), >100 (valeronitrile, silica film) and 162 (benzonitrile, Zirconia film) including the possibility to modify the surface into a hydrophobic state for repelling water. Finally, a wide variety of other plasmonic (bio-)sensors have been realized. Rodrigo et al. demonstrate a tunable nanostructured graphene biosensor for label-free protein monolayer detection (Rodrigo et al., 2015). Similar protein monolayers were investigated by Wu et al., exploiting multipixel arrays of Fano-resonant asymmetric metamaterials (FRAMMs) (Wu et al., 2012). More work on Fano-resonances in nanoscale plasmonic geometries can e.g., be found by Giannini et al. (2011). The field of nanophotonic biosensors using evanescent-field sensing in plasmonic metal-resonances and Mie resonances in dielectrics for label-free detection was recently reviewed by Altug et al. (2022). Kumar et al. (2018) instead give a review of the field of novel biosensor platforms for water-borne pathogen analysis using e.g., SPR concepts and more.

5.3 Mid-IR liquid sensing on the chip-scale

The previously discussed concepts demonstrate impressive results with respect to sensor specificity, sensitivity and in parts to compactness. Still, the resulting setups are regularly rather bulky with external (laser) light sources and thus still often yield time consuming offline measurements. This poses a strong limitation for applications in the analysis of dynamical processes in liquids such as chemical reactions (Norahan et al., 2021). The full monolithic integration of QCL, DL-plasmonic interaction section and QCD into a lab-on-a-chip sensor is a breakthrough solution that was realized by Schwarz et al. (2014); Ristanic et al. (2015) and recently used for *in situ* real-time monitoring of BSA (by Hinkov et al.) (Hinkov et al., 2022) and of an organic solvent by Pilat et al. (2023). It is summarized in Figure 2. Most recent work shows, that the plasmonic waveguides can be further improved, including: i) increased bandwidth in Ge-SLSPPs covering a full octave between 5.6–11.2 μm wavelength (David et al., 2021), ii) implementation of surface passivation coatings for protection from damaging liquids (David et al., 2023a), iii) surface functionalization for chemically specific enrichment and improved sensing of liquids (David et al., 2023a) and iv) on-chip plasmonic mode guiding based on novel polymeric materials like polyethylene (David et al., 2022; David et al., 2023b).

6 Discussion

Future developments in the field of plasmon-enhanced mid-IR liquid sensing are expected to further pursue chip-scale concepts. Particular current work in this field includes the realization of much

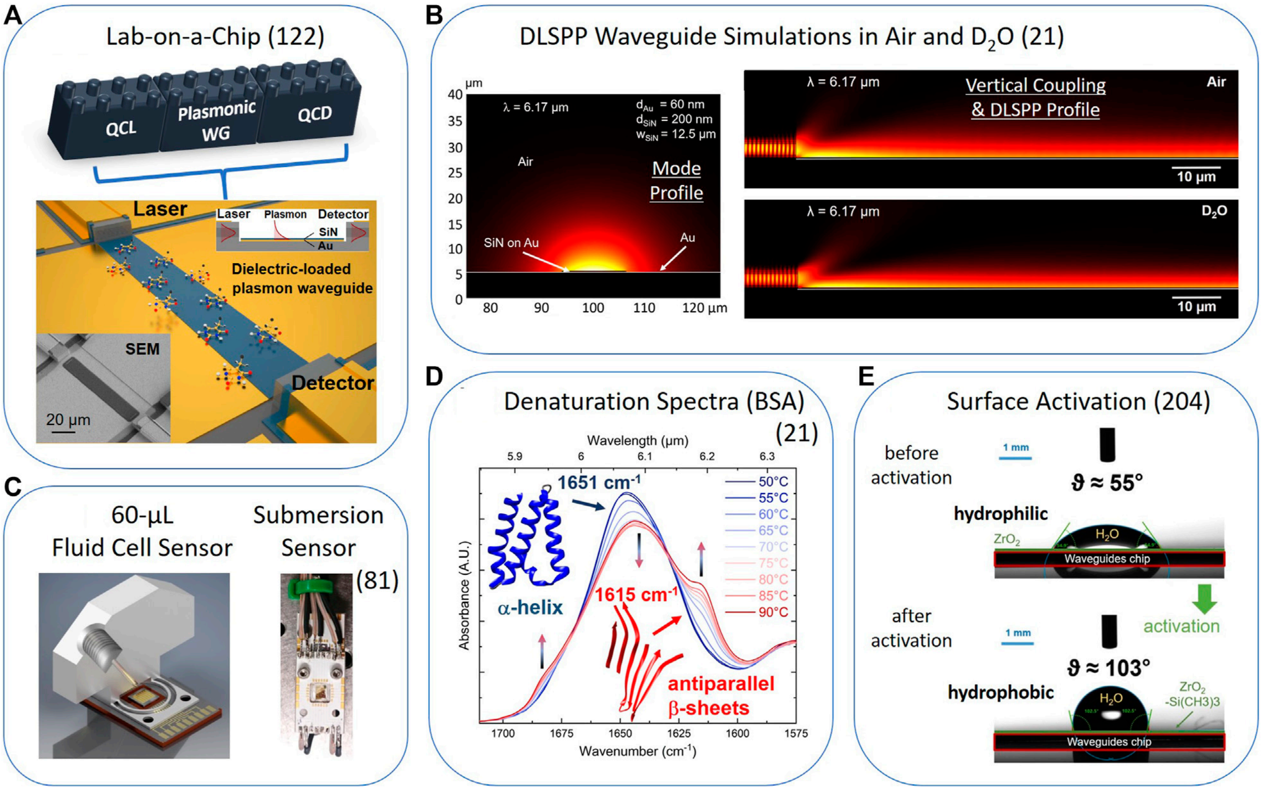

FIGURE 2
Overview over the application of the fully monolithic QC-technology based lab-on-a-chip concept. **(A)** Linear lab-on-a-chip concept based on QC technology and DLSPP waveguides. **(B)** DLSPP waveguide FEM-simulations for a SiN/Au configuration with the commercial software Comsol Multiphysics 5.5: (left) mode profile in air and (right) vertical coupling and DLSPP profile in air or D_2O. **(C)** (left) Design of a 60-μL fluid cell. (right) Picture of a submersion sensor configuration: the sensor chip is the golden square soldered in the middle of the white PCB. **(D)** Thermal denaturation spectra of the model protein BSA investigated between 1,575 and 1700 cm^{-1} and for temperatures between 50°C and 90°C with an ATR-FTIR sensor. **(E)** Contact angle measurements of water drops on a non-activated (top, hydrophilic, 3 μL, ϑ <90°) and activated (bottom, hydrophobic, 7 μL, ϑ >90°) ZrO_2-coated SLSPP waveguide surface. Figure **(A)** Adapted with permission from Schwarz et al., Nature Communications 5, 4,085, 2014; DOI: https://doi.org/10.1038/ncomms5085; licensed under CC BY-NC-SA 3.0. Figures **(B)** and **(D)** reproduced under CC-BY 4.0, Hinkov et al. (2022). Figure **(C)** reproduced from Pilat et al.(2023), licensed under CC BY 4.0 with permission from the Royal Society of Chemistry. Figure **(E)** reproduced under CC-BY 4.0, from arXiv2305.16522 [physics.optics].

more complex mid-IR PICs and photonic networks by implementing mode guiding and beam manipulating capabilities, similar to near-IR photonics (Soref, 2006). This will allow a much better beam steering control in the mid-IR as observed in free-space geometries (Hinkov et al., 2008). The novel on-chip concepts will potentially enable highly-sensitive plasmonic on-chip interferometers, e.g., in a "Mach-Zehnder" configuration or other heterodyne concepts which strongly benefit from miniaturized sensors. Furthermore, the implementation of plasmonic structures allowing single-molecule detection (Celebrano et al., 2011) or of microfluidic capabilities through polymer-based, on-chip structures, will additionally boost the use of such monolithic liquid sensors (Schwarz et al., 2014; Hinkov et al., 2022). The implementation of those new capabilities will open the pathway towards real-life sensing applications in disease monitoring, such as measuring specific protein-marker configurations as early diagnostic indicators for Parkinson's disease and other health conditions that can be monitored through body-fluid analysis. This can go as far as including *in vivo* bio-sensing applications (Pleitez et al., 2013; Pleitez Rafael et al., 2013) and enable the realization of the next-generation of commercial sensors based on fully integrated fingertip-sized geometries.

Author contributions

BH wrote the manuscript with editorial input from MD, GS, BS, and BL. All authors contributed to technical discussions and commented on the paper. All authors contributed to the article and approved the submitted version.

Funding

BH, MD and GS received funding from the EU Horizon 2020 Framework Program (project cFlow, No. 828893). BH acknowledges funding by the Austrian Science Fund FWF (M2485-N34). BH, GS and BL acknowledge financial support from the EU Horizion 2020 Framework Program (project

REDFINCH, No. 780240). BS received funding from the European Research Council (ERC) under the European Union's Horizon 2020 research and innovation program (Grant agreement No. 853014). BL acknowledges financial support from the European Union's research and innovation programme Horizon 2020 and Horizon Europe (projects AQUARIUS, No. 731465; HYDROPTICS, No. 71529; M3NIR, No. 101093008; BROMEDIR, No. 101092697).

Acknowledgments

Fruitful discussions with H. Detz, F. Pilat, W. Schrenk and E. Gornik and expert technical assistance by A. Linzer are greatly acknowledged.

Conflict of interest

The authors declare that the research was conducted in the absence of any commercial or financial relationships that could be construed as a potential conflict of interest.

Publisher's note

All claims expressed in this article are solely those of the authors and do not necessarily represent those of their affiliated organizations, or those of the publisher, the editors and the reviewers. Any product that may be evaluated in this article, or claim that may be made by its manufacturer, is not guaranteed or endorsed by the publisher.

References

Akhgar, C. K., Ramer, G., Zbik, M., Trajnerowicz, A., Pawluczyk, J., Schwaighofer, A., et al. (2020). The next generation of IR spectroscopy: EC-QCL-based mid-IR transmission spectroscopy of proteins with balanced detection. *Anal. Chem.* 92, 9901–9907. doi:10.1021/acs.analchem.0c01406

Altug, H., Oh, S. H., Maier, S. A., and Homola, J. (2022). Advances and applications of nanophotonic biosensors. *Nat. Nanotechnol.* 17, 5–16. doi:10.1038/s41565-021-01045-5

Amenabar, I., Poly, S., Nuansing, W., Hubrich, E. H., Govyadinov, A. A., Huth, F., et al. (2013). Structural analysis and mapping of individual protein complexes by infrared nanospectroscopy. *Nat. Commun.* 4, 2890. doi:10.1038/ncomms3890

Amrania, H., Antonacci, G., Chan, C. H., Drummond, L., Otto, W. R., Wright, N. A., et al. (2012). Digistain: A digital staining instrument for histopathology. *Opt. Express* 20, 7290. doi:10.1364/oe.20.007290

Amrania, H., Woodley-Barker, L., Goddard, K., Rosales, B., Shousha, S., Thomas, G., et al. (2018). Mid-infrared imaging in breast cancer tissue: An objective measure of grading breast cancer biopsies. *Converg. Sci. Phys. Oncol.* 4, 025001. doi:10.1088/2057-1739/aaabc3

Aroca, R. F., Ross, D. J., and Domingo, C. (2004). Surface-enhanced infrared spectroscopy. *Appl. Spectrosc.* 58, 324–338. doi:10.1366/0003702042475420

ASTM D6304 – 16 (2021). (Standard test method for determination of water in petroleum products, lubricating oils, and additives by coulometric karl fischer titration); AOCS official method ea 8-58, reapproved 2009 moisture, karl fischer volumetric method. Available at: https://www.astm.org/d6304-20.html.

Augel, L., Fischer, I. A., Hornung, F., Dressel, M., Berrier, A., Oehme, M., et al. (2016). Ellipsometric characterization of doped $Ge_{0.95}Sn_{0.05}$ films in the infrared range for plasmonic applications. *Opt. Lett.* 41, 4398–4400. doi:10.1364/ol.41.004398

Bai, Y., Bandyopadhyay, N., Tsao, S., Slivken, S., and Razeghi, M. (2011). Room temperature quantum cascade lasers with 27% wall plug efficiency. *Appl. Phys. Lett.* 98, 181102–181105. doi:10.1063/1.3586773

Baker, M. J., Trevisian, J., Bassan, P., Bhargava, R., Buttler, H. J., Dorling, K. M., et al. (2014). Using Fourier transform IR spectroscopy to analyze biological materials. *Nat. Protoc.* 9, 1771–1791. doi:10.1038/nprot.2014.110

Baldassarre, L., Giliberti, V., Rosa, A., Ortolani, M., Bonamore, A., Baiocco, P., et al. (2016). Mapping the amide I absorption in single bacteria and mammalian cells with resonant infrared nanospectroscopy. *Nanotechnology* 27, 075101. doi:10.1088/0957-4484/27/7/075101

Baldassarre, L., Sakat, E., Frigerio, J., Samarelli, A., Gallacher, K., Calandrini, E., et al. (2015). Midinfrared plasmon-enhanced spectroscopy with germanium antennas on silicon substrates. *Nano Lett.* 15, 7225–7231. doi:10.1021/acs.nanolett.5b03247

Bardeen, J., and Brattain, W. H. (1948). The transistor, A semiconductor triode. *Phys. Rev.* 74, 29–30. doi:10.1109/JPROC.1998.658753

Barelli, M., Giordano, M. C., Gucciardi, P. G., and Buatier De Mongeot, F. (2020). Self-organized nanogratings for large-area surface plasmon polariton excitation and surface-enhanced Raman spectroscopy sensing. *ACS Appl. Nano Mat.* 3, 8784–8793. doi:10.1021/acsanm.0c01569

Barker, A. S. (1968). Dielectric dispersion and phonon line shape in gallium phosphide. *Phys. Rev.* 165, 917–922. doi:10.1103/PhysRev.165.917

Barnes, W. L., Dereux, A., and Ebbesen, T. W. (2003). Surface plasmon subwavelength optics. *Nature* 424, 824–830. doi:10.1038/nature01937

Barreca, D., Laganà, G., Ficarra, S., Tellone, E., Leuzzi, U., Magazù, S., et al. (2010). Anti-aggregation properties of trehalose on heat-induced secondary structure and conformation changes of bovine serum albumin. *Biophys. Chem.* 147, 146–152. doi:10.1016/j.bpc.2010.01.010

Bartalini, S., Borri, S., Galli, I., Giusfredi, G., Mazzotti, D., Edamura, T., et al. (2011). Measuring frequency noise and intrinsic linewidth of a room-temperature DFB quantum cascade laser. *Opt. Express* 19, 17996. doi:10.1364/OE.19.017996

Barth, A., and Zscherp, C. (2002). What vibrations tell about proteins. *Q. Rev. Biophys.* 35, 369–430. doi:10.1017/S0033583502003815

Barth, A. (2007). Infrared spectroscopy of proteins. *Biochim. Biophys. Acta* 1767, 1073–1101. doi:10.1016/j.bbabio.2007.06.004

Bartlome, R., and Sigrist, M. W. (2009). Laser-based human breath analysis: D/H isotope ratio increase following heavy water intake. *Opt. Lett.* 34, 866–868. doi:10.1364/OL.34.000866

Baumgartner, B., Hayden, J., Loizillon, J., Steinbacher, S., Grosso, D., and Lendl, B. (2019). Pore size-dependent structure of confined water in mesoporous silica films from water adsorption/desorption using ATR-FTIR spectroscopy. *Langmuir* 35, 11986–11994. doi:10.1021/acs.langmuir.9b01435

Baumgartner, B., Hayden, J., Schwaighofer, A., and Lendl, B. (2018). *In situ* IR spectroscopy of mesoporous silica films for monitoring adsorption processes and trace analysis. *ACS Appl. Nano Mat.* 1, 7083–7091. doi:10.1021/acsanm.8b01876

Biagioni, P., Huang, J. S., and Hecht, B. (2012). Nanoantennas for visible and infrared radiation. *Rep. Prog. Phys.* 75, 024402. doi:10.1088/0034-4885/75/2/024402

Bibikova, O., Haas, J., López-Lorente, Á. I., Popov, A., Kinnunen, M., Ryabchikov, Y., et al. (2017). Surface enhanced infrared absorption spectroscopy based on gold nanostars and spherical nanoparticles. *Anal. Chim. Acta* 990, 141–149. doi:10.1016/j.aca.2017.07.045

Bismuto, A., Riedi, S., Hinkov, B., Beck, M., and Faist, J. (2012). Sb-free quantum cascade lasers in the 3 to 4 μm spectral range. *Semicond. Sci. Technol.* 27, 045013. doi:10.1088/0268-1242/27/4/045013

Brandstetter, M., Genner, A., Anic, K., and Lendl, B. (2010). Tunable external cavity quantum cascade laser for the simultaneous determination of glucose and lactate in aqueous phase. *Analyst* 135, 3260–3265. doi:10.1039/c0an00532k

Broudy, R. M., and Mazurczyk, V. J. (1981). Chapter 5 (HgCd)Te photoconductive detectors. *Semicond. Semimetals* 18, 157–199. doi:10.1016/S0080-8784(08)62765-9

Castellano, E. M. (2022). *Transparent conductive oxide plasmonics for the infrared* (United States: Wiley Online Library). PhD thesis.

Celebrano, M., Kukura, P., Renn, A., and Sandoghdar, V. (2011). Single-molecule imaging by optical absorption. *Nat. Photonics* 5, 95–98. doi:10.1038/nphoton.2010.290

Celebrano, M., Rocco, D., Gandolfi, M., Zilli, A., Rusconi, F., Tognazzi, A., et al. (2021). Optical tuning of dielectric nanoantennas for thermo-optically reconfigurable nonlinear metasurfaces. *Opt. Lett.* 46, 2453–2456. doi:10.1364/ol.420790

Celebrano, M., Wu, X., Baselli, M., Großmann, S., Biagioni, P., Locatelli, A., et al. (2015). Mode matching in multiresonant plasmonic nanoantennas for enhanced second harmonic generation. *Nat. Nanotechnol.* 10, 412–417. doi:10.1038/nnano.2015.69

CFA (2023). Hitran. Available at: https://www.cfa.harvard.edu/hitran/.

Cho, J., Park, J. H., Kim, J. K., and Schubert, E. F. (2017). White light-emitting diodes: History, progress, and future. *Laser Photonics Rev.* 11, 1600147. doi:10.1002/lpor.201600147

Chowdhury, D., Giordano, M. C., Manzato, G., Chittofrati, R., Mennucci, C., and Buatier De Mongeot, F. (2020). Large-area microfluidic sensors based on flat-optics Au nanostripe metasurfaces. *J. Phys. Chem. C* 124, 17183–17190. doi:10.1021/acs.jpcc.0c03023

Consolino, L., Nafa, M., De Regis, M., Cappelli, F., Garrasi, K., Mezzapesa, F. P., et al. (2020). Quantum cascade laser based hybrid dual comb spectrometer. *Commun. Phys.* 3, 69–9. doi:10.1038/s42005-020-0344-0

Constant, T. J., Hornett, S. M., Chang, D. E., and Hendry, E. (2016). All-optical generation of surface plasmons in graphene. *Nat. Phys.* 12, 124–127. doi:10.1038/nphys3545

Curl, R. F., Capasso, F., Gmachl, C., Kosterev, A. A., McManus, B., Lewicki, R., et al. (2010). Quantum cascade lasers in chemical physics. *Chem. Phys. Lett.* 487, 1–18. doi:10.1016/j.cplett.2009.12.073

Dabrowska, A., David, M., Freitag, S., Andrews, A. M., Strasser, G., Hinkov, B., et al. (2022). Broadband laser-based mid-infrared spectroscopy employing a quantum cascade detector for milk protein analysis. *Sensors Actuators B Chem.* 350, 130873. doi:10.1016/j.snb.2021.130873

David, M., Dabrowska, A., Sistani, M., Doganlar, I., Hinkelmann, E., Detz, H., et al. (2021). Octave-spanning low-loss mid-IR waveguides based on semiconductor-loaded plasmonics. *Opt. Express* 29, 43567–43579. doi:10.1364/OE.443966

David, M., Disnan, D., Arigliani, E., Lardschneider, E., Marschick, G., Hoang, H. T., et al. (2023b). Advanced mid-infrared plasmonic waveguides based on polymers for on-chip integrated photonics. arXiv:2305.03586 [physics.optics]. doi:10.48550/arXiv.2305.03586

David, M., Disnan, D., Lardschneider, A., Wacht, D., Hoang, H. T., Ramer, G., et al. (2022). Structure and mid-infrared optical properties of spin-coated polyethylene films developed for integrated photonics applications. *Opt. Mat. Express* 12, 2168. doi:10.1364/ome.458667

David, M., Doganlar, I. C., Nazzari, D., Arigliani, E., Wacht, D., Sistani, M., et al. (2023a). Surface protection and activation of mid-IR plasmonic waveguides for spectroscopy of liquids. arXiv:2305.16522 [physics.optics]. doi:10.48550/arXiv.2305.16522

De La Arada, I., Seiler, C., and Mäntele, W. (2012). Amyloid fibril formation from human and bovine serum albumin followed by quasi-simultaneous Fourier-transform infrared (FT-IR) spectroscopy and static light scattering (SLS). *Eur. Biophys. J.* 41, 931–938. doi:10.1007/s00249-012-0845-1

De Meutter, J., and Goormaghtigh, E. (2021). Evaluation of protein secondary structure from FTIR spectra improved after partial deuteration. *Eur. Biophys. J.* 50, 613–628. doi:10.1007/s00249-021-01502-y

Delga, A. (2020). Quantum cascade detectors: A review. *Mid-infrared Optoelectron. Mat. Devices, Appl. Chap.* 8, 337–377. doi:10.1016/B978-0-08-102709-7.00008-5

Dely, H., Bonazzi, T., Spitz, O., Rodriguez, E., Gacemi, D., Todorov, Y., et al. (2022). 10 Gbit s^{-1} free space data transmission at 9 μm wavelength with unipolar quantum optoelectronics. *Laser Photonics Rev.* 16, 2100414–2100417. doi:10.1002/lpor.202100414

Di Francescantonio, A., Locatelli, A., Wu, X., Zilli, A., Feichtner, T., Biagioni, P., et al. (2022). Coherent control of the nonlinear emission of single plasmonic nanoantennas by dual-beam pumping. *Adv. Opt. Mat.* 10, 2200757. doi:10.1002/adom.202200757

Ebbesen, T. W., Lezec, H. J., Ghaemi, H. F., Thio, T., and Wolff, P. A. (1998). Extraordinary optical transmission through sub-wavelength hole arrays. *Nature* 391, 667–669. doi:10.1038/35570

Ehlers, D. H., and Mills, D. L. (1987). Surface plasmons on n-type semiconductors: Influence of depletion and accumulation layers. *Phys. Rev. B* 36, 1051–1067. doi:10.1103/physrevb.36.1051

EPA (2014). Global greenhouse gas emissions data. Available at: https://www.epa.gov/ghgemissions/global-greenhouse-gas-emissions-data.

Fabian, H., and Mäntele, W. (2006). Infrared spectroscopy of proteins. *B. Handb. Vib. Spectrosc.* 2006. doi:10.1002/0470027320.s8201

Faist, J., Capasso, F., Sivco, D. L., Sirtori, C., Hutchinson, A. L., and Cho, A. Y. (1994). Quantum cascade laser. *Sci. (80-.)* 264, 553–556. doi:10.1126/science.264.5158.553

Faist, J., Gmachl, C., Capasso, F., Sirtori, C., Sivco, D. L., Baillargeon, J. N., et al. (1997). Distributed feedback quantum cascade lasers. *Appl. Phys. Lett.* 70, 2670–2672. doi:10.1063/1.119208

Faist, J. (2013). *Quantum cascade lasers*. Oxford, United Kingdom: Oxford Univ. Press, 318. doi:10.1093/acprof:oso/9780198528241.001.0001

Falk, A. L., Koppens, F. H. L., Yu, C. L., Kang, K., De Leon Snapp, N., Akimov, A. V., et al. (2009). Near-field electrical detection of optical plasmons and single-plasmon sources. *Nat. Phys.* 5, 475–479. doi:10.1038/nphys1284

Fei, Z., Rodin, A. S., Andreev, G. O., Bao, W., McLeod, A. S., Wagner, M., et al. (2012). Gate-tuning of graphene plasmons revealed by infrared nano-imaging. *Nature* 487, 82–85. doi:10.1038/nature11253

Flannigan, L., Yoell, L., and Xu, C. Q. (2022). Mid-wave and long-wave infrared transmitters and detectors for optical satellite communications - a review. *J. Opt.* 24, 043002. doi:10.1088/2040-8986/ac56b6

Fleischmann, M., Hendra, P. J., and McQuillan, A. J. (1974). Raman spectra of pyridine adsorbed at a silver electrode. *Chem. Phys. Lett.* 26, 163–166. doi:10.1016/0009-2614(74)85388-1

Frank, F., Baumgartner, B., David, M., Doganlar, I. C., Strasser, G., Hinkov, B., et al. (2021). "Development of a nanomolar sensitivity dipstick mid-IR ATR sensor for phosphate in water," in 11th Int. Conf. Adv. Vib. Spectrosc., Krakow, Poland, Aug 23–26 2021. Available at: https://www.ise.fraunhofer.de/en/press-media/press-releases/2022/fraunhofer-ise-develops-the-worlds-most-efficient-solar-cell-with-47-comma-6-percent-efficiency.html.

Fraunhofer-ISE (2022). Fraunhofer ISE develops world's most efficient solar cell with 47.6 percent efficiency. *Fraunhofer-ISE* 2022.

Frigerio, J., Ballabio, A., Isella, G., Sakat, E., Pellegrini, G., Biagioni, P., et al. (2016). Tunability of the dielectric function of heavily doped germanium thin films for mid-infrared plasmonics. *Phys. Rev. B* 94, 085202. doi:10.1103/PhysRevB.94.085202

Fuchs, F., Hinkov, B., Hugger, S., Kaster, J. M., Aidam, R., Bronner, W., et al. (2010). Imaging stand-off detection of explosives using tunable MIR quantum cascade lasers. *Proc. SPIE* 7608. doi:10.1117/12.840464

Garcia-Perez, M., Wang, S., Shen, J., Rhodes, M., Lee, W. J., and Li, C. Z. (2008). Effects of temperature on the formation of lignin-derived oligomers during the fast pyrolysis of Mallee woody biomass. *Energy Fuels* 22, 2022–2032. doi:10.1021/ef7007634

Giannini, V., Francescato, Y., Amrania, H., Phillips, C. C., and Maier, S. A. (2011). Fano resonances in nanoscale plasmonic systems: A parameter-free modeling approach. *Nano Lett.* 11, 2835–2840. doi:10.1021/nl201207n

Ginn, J. C., Jarecki, R. L., Shaner, E. A., and Davids, P. S. (2011). Infrared plasmons on heavily-doped silicon. *J. Appl. Phys.* 110, 043110. doi:10.1063/1.3626050

Golosovsky, M., Lirtsman, V., Yashunsky, V., Davidov, D., and Aroeti, B. (2009). Midinfrared surface-plasmon resonance: A novel biophysical tool for studying living cells. *J. Appl. Phys.* 105, 102036. doi:10.1063/1.3116143

Gómez Rivas, J., Kuttge, M., Haring Bolivar, P., Kurz, H., and Sánchez-Gil, J. A. (2004). Propagation of surface plasmon polaritons on semiconductor gratings. *Phys. Rev. Lett.* 93, 256804. doi:10.1103/PhysRevLett.93.256804

Grigorenko, A. N., Polini, M., and Novoselov, K. S. (2012). Graphene plasmonics. *Nat. Photonics* 6, 749–758. doi:10.1038/nphoton.2012.262

Güler, G., Vorob'ev, M. M., Vogel, V., and Mäntele, W. (2016). Proteolytically-induced changes of secondary structural protein conformation of bovine serum albumin monitored by Fourier transform infrared (FT-IR) and UV-circular dichroism spectroscopy. *Spectrochim. Acta - Part A Mol. Biomol. Spectrosc.* 161, 8–18. doi:10.1016/j.saa.2016.02.013

Guo, X., Ma, Y., Wang, Y., and Tong, L. (2013). Nanowire plasmonic waveguides, circuits and devices. *Laser Photonics Rev.* 7, 855–881. doi:10.1002/lpor.201200067

Haas, J., and Mizaikoff, B. (2016). Advances in mid-infrared spectroscopy for chemical analysis. *Annu. Rev. Anal. Chem.* 9, 45–68. doi:10.1146/annurev-anchem-071015-041507

Hall, R. N., Fenner, G. E., Kingsley, J. D., Soltys, T. J., and Carlson, R. O. (1962). Coherent light emission from GaAs junctions. *Phys. Rev. Lett.* 9, 366–368. doi:10.1103/PhysRevLett.9.366

Harima, H., Sakashita, H., and Nakashima, S. (1998). Raman microprobe measurement of under-damped LO-phonon-plasmon coupled mode in n-type GaN. *Mat. Sci. Forum* 264-268, 1363–1366. doi:10.4028/www.scientific.net/msf.264-268.1363

Hartstein, A., Kirtley, J. R., and Tsang, J. C. (1980). Enhancement of the infrared absorption from molecular monolayers with thin metal overlayers. *Phys. Rev. Lett.* 45, 201–204. doi:10.1103/PhysRevLett.45.201

Hatta, A., Suzuki, Y., and Suëtaka, W. (1984). Infrared absorption enhancement of monolayer species on thin evaporated Ag films by use of a Kretschmann configuration: Evidence for two types of enhanced surface electric fields. *Appl. Phys. A* 35, 135–140. doi:10.1007/BF00616965

Hinkov, B., Beck, M., Gini, E., and Faist, J. (2013). Quantum cascade laser in a master oscillator power amplifier configuration with Watt-level optical output power. *Opt. Express* 21, 19180–19186. doi:10.1364/oe.21.019180

Hinkov, B., Bismuto, A., Bonetti, Y., Beck, M., Blaser, S., and Faist, J. (2012). Singlemode quantum cascade lasers with power dissipation below 1 W. *Electron. Lett.* 48, 646. doi:10.1049/el.2012.1204

Hinkov, B., Fuchs, F., Bronner, W., Köhler, K., and Wagner, J. (2008). Current- and temperature-induced beam steering in 7.8-${\mu}$m emitting quantum-cascade lasers. *IEEE J. Quantum Electron.* 44, 1124–1128. doi:10.1109/jqe.2008.2003499

Hinkov, B., Fuchs, F., Kaster, J. M., Yang, Q., Bronner, W., Aidam, R., et al. (2009). Broad band tunable quantum cascade lasers for stand-off detection of explosives. *Proc. SPIE* 7484, 748406. doi:10.1117/12.830358

Hinkov, B., Fuchs, F., Yang, Q. K., Kaster, J. M., Bronner, W., Aidam, R., et al. (2010). Time-resolved spectral characteristics of external-cavity quantum cascade lasers and their application to stand-off detection of explosives. *Appl. Phys. B Lasers Opt.* 100, 253–260. doi:10.1007/s00340-009-3863-7

Hinkov, B., Hayden, J., Szedlak, R., Martin-Mateos, P., Jerez, B., Acedo, P., et al. (2019). High frequency modulation and (quasi) single-sideband emission of mid-infrared ring and ridge quantum cascade lasers. *Opt. Express* 27, 14716–14724. doi:10.1364/oe.27.014716

Hinkov, B., Hugi, A., Beck, M., and Faist, J. (2016). Rf-modulation of mid-infrared distributed feedback quantum cascade lasers. *Opt. Express* 24, 3294. doi:10.1364/OE.24.003294

Hinkov, B., Pilat, F., Lux, L., Souza, P. L., David, M., Schwaighofer, A., et al. (2022). A mid-infrared lab-on-a-chip for dynamic reaction monitoring. *Nat. Commun.* 13, 4753. doi:10.1038/s41467-022-32417-7

Hoffman, F. M. (1983). Infrared reflection absorption spectroscopy of adsorbed molecules. *Surf. Sci. Rep.* 3, 107–192. doi:10.1016/0167-5729(83)90001-8

Hofstetter, D., Beck, M., and Faist, J. (2002). Quantum-cascade-laser structures as photodetectors. *Appl. Phys. Lett.* 81, 2683–2685. doi:10.1063/1.1512954

Holmgaard, T., and Bozhevolnyi, S. I. (2007). Theoretical analysis of dielectric-loaded surface plasmon-polariton waveguides. *Phys. Rev. B - Condens. Matter Mat. Phys.* 75, 245405–245412. doi:10.1103/PhysRevB.75.245405

Homola, J. (2006). Surface plasmon resonance based sensors. *Springer Ser. Chem. Sensors Biosens.* Springer-Verlag Berlin 4, 1–251. doi:10.1007/b100321

Huang, J. A., and Luo, L. B. (2018). Low-Dimensional plasmonic photodetectors: Recent progress and future opportunities. *Adv. Opt. Mat.* 6, 1701282–1701318. doi:10.1002/adom.201701282

Huang, L., Luo, R., Liu, X., and Hao, X. (2022). Spectral imaging with deep learning. *Light Sci. Appl.* 11, 61. doi:10.1038/s41377-022-00743-6

Huang, Y., Hsiang, E. L., Deng, M. Y., and Wu, S. T. (2020). Mini-LED, micro-LED and OLED displays: Present status and future perspectives. *Light Sci. Appl.* 9, 105. doi:10.1038/s41377-020-0341-9

Hugi, A., Terazzi, R., Bonetti, Y., Wittmann, A., Fischer, M., Beck, M., et al. (2009). External cavity quantum cascade laser tunable from 7.6 to 11.4 μm. *Appl. Phys. Lett.* 95, 061103–061130. doi:10.1063/1.3193539

IPCC (2022). IPCC report on climate change 2022 - mitigation of climate change. Available at: https://www.ipcc.ch/report/ar6/wg3/downloads/report/IPCC_AR6_WGIII_FullReport.pdf.

Jollivet, A., Hinkov, B., Pirotta, S., Hoang, H., Derelle, S., Jaeck, J., et al. (2018). Short infrared wavelength quantum cascade detectors based on m-plane ZnO/ZnMgO quantum wells. *Appl. Phys. Lett.* 113, 251104. doi:10.1063/1.5058120

Jouy, P., Bonzon, C., Wolf, J., Gini, E., Beck, M., and Faist, J. (2015). Surface emitting multi-wavelength array of single frequency quantum cascade lasers. *Appl. Phys. Lett.* 106, 071104. doi:10.1063/1.4913203

Kerstel, E. (2003). *CHAPTER 34 isotope ratio infrared spectrometry*.

Kilgus, J., Langer, G., Duswald, K., Zimmerleiter, R., Zorin, I., Berer, T., et al. (2018). Diffraction limited mid-infrared reflectance microspectroscopy with a supercontinuum laser. *Opt. Express* 26, 30644. doi:10.1364/oe.26.030644

Kischkat, J., Peters, S., Gruska, B., Semtsiv, M., Chashnikova, M., Klinkmüller, M., et al. (2012). Mid-infrared optical properties of thin films of aluminum oxide, titanium dioxide, silicon dioxide, aluminum nitride, and silicon nitride. *Appl. Opt.* 51, 6789–6798. doi:10.1364/AO.51.006789

Knötig, H., Hinkov, B., Weih, R., Höfling, S., Koeth, J., and Strasser, G. (2020). Continuous-wave operation of vertically emitting ring interband cascade lasers at room temperature. *Appl. Phys. Lett.* 116, 131101. doi:10.1063/1.5139649

Komagata, K. N., Wittwer, V. J., Südmeyer, T., Emmenegger, L., and Gianella, M. (2023). Absolute frequency referencing for swept dual-comb spectroscopy with midinfrared quantum cascade lasers. *Phys. Rev. Res.* 5, 013047. doi:10.1103/physrevresearch.5.013047

Kosterev, A., Wysocki, G., Bakhirkin, Y., So, S., Lewicki, R., Fraser, M., et al. (2008). Application of quantum cascade lasers to trace gas analysis. *Appl. Phys. B Lasers Opt.* 90, 165–176. doi:10.1007/s00340-007-2846-9

Krasavin, A. V., and Zayats, A. V. (2015). Active nanophotonic circuitry based on dielectric-loaded plasmonic waveguides. *Adv. Opt. Mat.* 3, 1662–1690. doi:10.1002/adom.201500329

Kumar, A., Gosciniak, J., Volkov, V. S., Papaioannou, S., Kalavrouziotis, D., Vyrsokinos, K., et al. (2013). Dielectric-loaded plasmonic waveguide components: Going practical. *Laser Phot. Rev.* 7, 938–951. doi:10.1002/lpor.201200113

Kumar, N., Hu, Y., Singh, S., and Mizaikoff, B. (2018). Emerging biosensor platforms for the assessment of water-borne pathogens. *Analyst* 143, 359–373. doi:10.1039/c7an00983f

Kushiyama, Y., Arima, T., and Uno, T. (2012). Experimental verification of spoof surface plasmons in wire metamaterials. *Opt. Express* 20, 18238. doi:10.1364/OE.20.018238

Lal, S., Link, S., and Halas, N. J. (2007). Nano-optics from sensing to waveguiding. *Nat. Photonics* 1, 641–648. doi:10.1038/nphoton.2007.223

Langer, J., de Aberasturi, D. J., Aizpurua, J., Alvarez-Puebla, R. A., Auguié, B., Baumberg, J. J., et al. (2020). Present and future of surface-enhanced Raman scattering. *ACS Nano* 14, 28–117. doi:10.1021/acsnano.9b04224

Law, S., Adams, D. C., Taylor, A. M., and Wasserman, D. (2012). Mid-infrared designer metals. *Opt. Express* 20, 12155–12165. doi:10.1364/OE.20.012155

Law, S., Podolskiy, V., and Wasserman, D. (2013). Towards nano-scale photonics with micro-scale photons: The opportunities and challenges of mid-infrared plasmonics. *Nanophotonics* 2, 103–130. doi:10.1515/nanoph-2012-0027

Levine, B. F., Choi, K. K., Bethea, C. G., Walker, J., and Malik, R. J. (1987). New 10 μm infrared detector using intersubband absorption in resonant tunneling GaAlAs superlattices. *Appl. Phys. Lett.* 50, 1092–1094. doi:10.1063/1.97928

Li, J. S., Chen, W., and Fischer, H. (2013). Quantum cascade laser spectrometry techniques: A new trend in atmospheric chemistry. *Appl. Spectrosc. Rev.* 48, 523–559. doi:10.1080/05704928.2012.757232

Li, J. V., Yang, R. Q., Hill, C. J., and Chuang, S. L. (2005). Interband cascade detectors with room temperature photovoltaic operation. *Appl. Phys. Lett.* 86, 101102–101103. doi:10.1063/1.1875758

Liu, H., and Lalanne, P. (2008). Microscopic theory of the extraordinary optical transmission. *Nature* 452, 728–731. doi:10.1038/nature06762

López-Lorente, Á. I., Wang, P., and Mizaikoff, B. (2017). Towards label-free mid-infrared protein assays: *In-situ* formation of bare gold nanoparticles for surface enhanced infrared absorption spectroscopy of bovine serum albumin. *Microchim. Acta* 184, 453–462. doi:10.1007/s00604-016-2031-0

Lu, L., Zhang, J., Xie, Y., Gao, F., Xu, S., Wu, X., et al. (2020). Wearable health devices in health care: Narrative systematic review. *JMIR Mhealth Uhealth* 8, e18907. doi:10.2196/18907

Lu, Q. Y., Bai, Y., Bandyopadhyay, N., Slivken, S., and Razeghi, M. (2011). 2.4 W room temperature continuous wave operation of distributed feedback quantum cascade lasers. *Appl. Phys. Lett.* 98, 181106. doi:10.1063/1.3588412

Lu, R., Li, W. W., Katzir, A., Raichlin, Y., Yu, H. Q., and Mizaikoff, B. (2015). Probing the secondary structure of bovine serum albumin during heat-induced denaturation using mid-infrared fiberoptic sensors. *Analyst* 140, 765–770. doi:10.1039/c4an01495b

Lyakh, A., Maulini, R., Tsekoun, A., Go, R., and Patel, C. K. N. (2012a). Multiwatt long wavelength quantum cascade lasers based on high strain composition with 70% injection efficiency. *Opt. Express* 20, 24272. doi:10.1364/OE.20.024272

Lyakh, A., Maulini, R., Tsekoun, A., Go, R., and Patel, C. K. N. (2012b). Tapered 4.7 μm quantum cascade lasers with highly strained active region composition delivering over 4.5 watts of continuous wave optical power. *Opt. Express* 20, 4382. doi:10.1364/OE.20.004382

Ma, Y., Hu, Y., Qiao, S., Lang, Z., Liu, X., He, Y., et al. (2022). Quartz tuning forks resonance frequency matching for laser spectroscopy sensing. *Photoacoustics* 25, 100329. doi:10.1016/j.pacs.2022.100329

Marschick, G., David, M., Arigliani, E., Opacak, N., Schwarz, B., Giparakis, M., et al. (2022). High-responsivity operation of quantum cascade detectors at 9 μm. *Opt. Express* 30, 40188. doi:10.1364/oe.470615

Marschick, G., Knötig, H., Weih, R., Koeth, J., Strasser, G., and Hinkov, B. (2023). Concentric double-ring interband cascade lasers for bi-color emission in continuous wave mode. *Proc. SPIE* 12440, PC1244009. doi:10.1117/12.2650784

Martín-Moreno, L., García-Vidal, F. J., Lezec, H. J., Pellerin, K. M., Thio, T., Pendry, J. B., et al. (2001). Theory of extraordinary optical transmission through subwavelength hole arrays. *Phys. Rev. Lett.* 86, 1114–1117. doi:10.1103/PhysRevLett.86.1114

Meyer, J. R., Bewley, W. W., Canedy, C. L., Kim, C. S., Kim, M., Merritt, C. D., et al. (2020). The interband cascade laser. *Photonics* 7, 75. doi:10.3390/PHOTONICS7030075

Mizaikoff, B. (2013). Waveguide-enhanced mid-infrared chem/bio sensors. *Chem. Soc. Rev.* 42, 8683–8699. doi:10.1039/c3cs60173k

Mousavi, Z., Naseri, M., Babaei, S., Hosseini, S. M. H., and Shekarforoush, S. S. (2021). The effect of cross-linker type on structural, antimicrobial and controlled release properties of fish gelatin-chitosan composite films incorporated with ϵ-poly-L-lysine. *Int. J. Biol. Macromol.* 183, 1743–1752. doi:10.1016/j.ijbiomac.2021.05.159

Mujagić, E., Schwarzer, C., Yao, Y., Chen, J., Gmachl, C., and Strasser, G. (2011). Two-dimensional broadband distributed-feedback quantum cascade laser arrays. *Appl. Phys. Lett.* 98, 141101. doi:10.1063/1.3574555

Murayama, K., and Tomida, M. (2004). Heat-induced secondary structure and conformation change of bovine serum albumin investigated by Fourier transform infrared spectroscopy. *Biochemistry* 43, 11526–11532. doi:10.1021/bi0489154

Nadiri, I. M., and Nandi, B. (2003). Telecommunications infrastructure and economic development. *Tradit. Telecommun. Netw.* 1, 293–314. doi:10.4337/9781781950630.00019

Naik, G. V., Shalaev, V. M., and Boltasseva, A. (2013). Alternative plasmonic materials: Beyond gold and silver. *Adv. Mat.* 25, 3264–3294. doi:10.1002/adma.201205076

Neubrech, F., Huck, C., Weber, K., Pucci, A., and Giessen, H. (2017). Surface-enhanced infrared spectroscopy using resonant nanoantennas. *Chem. Rev.* 117, 5110–5145. doi:10.1021/acs.chemrev.6b00743

Nie, S., and Emory, S. R. (1997). Probing single molecules and single nanoparticles by surface-enhanced Raman scattering. *Science* 275, 1102–1106. doi:10.1126/science.275.5303.1102

Nielsen, M. G., Bernardin, T., Hassan, K., Kriezis, E. E., and Weeber, J. C. (2014). Silicon-loaded surface plasmon polariton waveguides for nanosecond thermo-optical switching. *Opt. Lett.* 39, 2282. doi:10.1364/ol.39.002282

Norahan, M. J., Horvath, R., Woitzik, N., Jouy, P., Eigenmann, F., Gerwert, K., et al. (2021). Microsecond-resolved infrared spectroscopy on nonrepetitive protein reactions by applying caged compounds and quantum cascade laser frequency combs. *Anal. Chem.* 93, 6779–6783. doi:10.1021/acs.analchem.1c00666

N'tsame Guilengui, V., Cerutti, L., Rodriguez, J. B., Tournié, E., and Taliercio, T. (2012). Localized surface plasmon resonances in highly doped semiconductors nanostructures. *Appl. Phys. Lett.* 101, 161113. doi:10.1063/1.4760281

Osawa, M. (1997). *Dynamic processes in electrochemical reactions studied by surface-enhanced infrared absorption spectroscopy*. SEIRAS. doi:10.1246/bcsj.70.2861

Ozbay, E (2006). Plasmonics: Merging photonics and electronics at nanoscale dimensions. *Sci. (80-.)* 311, 189–193. doi:10.1126/science.1114849

Pang, X., Schatz, R., Joharifar, M., Udalcovs, A., Bobrovs, V., Zhang, L., et al. (2022). Direct modulation and free-space transmissions of up to 6 gbps multilevel signals with a 4.65-μm quantum cascade laser at room temperature. *J. Light. Technol.* 40, 2370–2377. doi:10.1109/JLT.2021.3137963

Patimisco, P., Sampaolo, A., Dong, L., Tittel, F. K., and Spagnolo, V. (2018). Recent advances in quartz enhanced photoacoustic sensing. *Appl. Phys. Rev.* 5, 011106. doi:10.1063/1.5013612

Patimisco, P., Scamarcio, G., Tittel, F. K., and Spagnolo, V. (2014). Quartz-enhanced photoacoustic spectroscopy: A review. *Sensors* 14, 6165–6206. doi:10.3390/s140406165

Pellegrini, G., Baldassare, L., Giliberti, V., Frigerio, J., Gallacher, K., Paul, D. J., et al. (2018). Benchmarking the use of heavily doped Ge for plasmonics and sensing in the mid-infrared. *ACS Photonics* 5, 3601–3607. doi:10.1021/acsphotonics.8b00438

Pendry, J. B., Martín-Moreno, L., and Garcia-Vidal, F. J. (2004). Mimicking surface plasmons with structured surfaces. *Science* 305, 847–848. doi:10.1126/science.1098999

Perry, D. A., Borchers, R. L., Golden, J. W., Owen, A. R., Price, A. S., Henry, W. A., et al. (2013). Surface-enhanced infrared absorption on elongated nickel nanostructures. *J. Phys. Chem. Lett.* 4, 3945–3949. doi:10.1021/jz402092y

Pilat, F., Schwarz, B., Baumgartner, B., Ristanić, D., Detz, H., Andrews, A. M., et al. (2023). Beyond karl fischer titration: A monolithic quantum cascade sensor for monitoring residual water concentration in solvents. *Lab. Chip* 23, 1816–1824. doi:10.1039/d2lc00724j

Pleitez, M. A., Lieblein, T., Bauer, A., Hertzberg, O., Von Lilienfeld-Toal, H., and Mäntele, W. (2013). Windowless ultrasound photoacoustic cell for*in vivo*mid-IR spectroscopy of human epidermis: Low interference by changes of air pressure, temperature, and humidity caused by skin contact opens the possibility for a non-invasive monitoring of glucose in the interstitial fluid. *Rev. Sci. Instrum.* 84, 084901. doi:10.1063/1.4816723

Pleitez Rafael, M. Á., Lieblein, T., Bauer, A., Hertzberg, O., von Lilienfeld-Toal, H., and Mäntele, W. (2013). *In vivo* noninvasive monitoring of glucose concentration in human epidermis by mid-infrared pulsed photoacoustic spectroscopy. *Anal. Chem.* 85, 1013–1020. doi:10.1021/ac302841f

Pushkarsky, M. B., Dunayevskiy, I. G., Prasanna, M., Tsekoun, A. G., Go, R., and Patel, C. K. N. (2006). High-sensitivity detection of TNT. *PNAS* 103, 19630–19634. doi:10.1073/pnas.0609789104

Raether, H. (1988). Surface plasmons on smooth and rough surfaces and on gratings. *Springer Tracts Mod. Phys.* 136. doi:10.1007/BFb0048317

Rauter, P., Menzel, S., Goyal, A. K., Wang, C. A., Sanchez, A., Turner, G., et al. (2013). High-power arrays of quantum cascade laser master-oscillator power-amplifiers. *Opt. Express* 21, 4518. doi:10.1364/OE.21.004518

Razeghi, M. (2020). InAs/GaSb type II superlattices: A developing material system for third generation of IR imaging. *Mid-infrared Optoelectron. Mat. Devices, Appl. Chap.* 9, 379–413. doi:10.1016/B978-0-08-102709-7.00009-7

Reininger, P., Schwarz, B., Harrer, A., Zederbauer, T., Detz, H., Andrews, A. M., et al. (2013). Photonic crystal slab quantum cascade detector. *Appl. Phys. Lett.* 103, 241103. doi:10.1063/1.4846035

Ricchiuti, G., Dabrowska, A., Pinto, D., Ramer, G., and Lendl, B. (2022). Dual-beam photothermal spectroscopy employing a Mach- Zehnder interferometer and an external cavity quantum cascade laser for detection of water traces in organic solvents. *Anal. Chem.* 94, 16353–16360. doi:10.1021/acs.analchem.2c03303

Riedi, S., Hugi, A., Bismuto, A., Beck, M., and Faist, J. (2013). Broadband external cavity tuning in the 3-4 μm window. *Appl. Phys. Lett.* 103, 031108. doi:10.1063/1.4813851

Ristanic, D., Schwarz, B., Reininger, P., Detz, H., Zederbauer, T., Andrews, A. M., et al. (2015). Monolithically integrated mid-infrared sensor using narrow mode operation and temperature feedback. *Appl. Phys. Lett.* 106, 041101. doi:10.1063/1.4906802

Rodrigo, D., Limaj, O., Janner, D., Etezadi, D., García De Abajo, F. J., Pruneri, V., et al. (2015). Mid-infrared plasmonic biosensing with graphene. *Sci. (80)* 349, 165–168. doi:10.1126/science.aab2051

Sarid, D. (1981). Long-range surface-plasma waves on very thin metal films. *Phys. Rev. Lett.* 47, 1927–1930. doi:10.1103/PhysRevLett.47.1927

Scheuermann, J., Weih, R., von Edlinger, M., Nähle, L., Fischer, M., Koeth, J., et al. (2015). Single-mode interband cascade lasers emitting below 2.8 μm. *Appl. Phys. Lett.* 106, 161103. doi:10.1063/1.4918985

Schwaighofer, A., Akhgar, C. K., and Lendl, B. (2021). Broadband laser-based mid-IR spectroscopy for analysis of proteins and monitoring of enzyme activity. *Spectrochim. Acta Part A Mol. Biomol. Spectrosc.* 253, 119563. doi:10.1016/j.saa.2021.119563

Schwaighofer, A., Alcaráz, M. R., Araman, C., Goicoechea, H., and Lendl, B. (2016). External cavity-quantum cascade laser infrared spectroscopy for secondary structure analysis of proteins at low concentrations. *Sci. Rep.* 6, 33556. doi:10.1038/srep33556

Schwaighofer, A., Brandstetter, M., and Lendl, B. (2017). Quantum cascade lasers (QCLs) in biomedical spectroscopy. *Chem. Soc. Rev.* 46, 5903–5924. doi:10.1039/c7cs00403f

Schwaighofer, A., and Lendl, B. (2020). Quantum cascade laser-based infrared transmission spectroscopy of proteins in solution. *Vib. Spectrosc. Protein Res.* 2020. 59–88. doi:10.1016/B978-0-12-818610-7.00003-7

Schwarz, B., Reininger, P., Ristanić, D., Detz, H., Andrews, A. M., Schrenk, W., et al. (2014). Monolithically integrated mid-infrared lab-on-a-chip using plasmonics and quantum cascade structures. *Nat. Commun.* 5, 4085. doi:10.1038/ncomms5085

Schwarz, B., Wang, C. A., Missaggia, L., Mansuripur, T. S., Chevalier, P., Connors, M. K., et al. (2017). Watt-Level continuous-wave emission from a bifunctional quantum cascade laser/detector. *ACS Photonics* 4, 1225–1231. doi:10.1021/acsphotonics.7b00133

Shrivastav, A. M., Cvelbar, U., and Abdulhalim, I. (2021). A comprehensive review on plasmonic-based biosensors used in viral diagnostics. *Commun. Biol.* 4, 70–12. doi:10.1038/s42003-020-01615-8

Sistani, M., Bartmann, M. G., Güsken, N. A., Oulton, R. F., Keshmiri, H., Luong, M. A., et al. (2020). Plasmon-driven hot electron transfer at atomically sharp metal-semiconductor nanojunctions. *ACS Photonics* 7, 1642–1648. doi:10.1021/acsphotonics.0c00557

Sistani, M., Bartmann, M. G., Güsken, N. A., Oulton, R. F., Keshmiri, H., Seifner, M. S., et al. (2019). Nanoscale aluminum plasmonic waveguide with monolithically integrated germanium detector. *Appl. Phys. Lett.* 115, 161107. doi:10.1063/1.5115342

Smuck, M., Odonkor, C. A., Wilt, J. K., Schmidt, N., and Swiernik, M. A. (2021). The emerging clinical role of wearables: Factors for successful implementation in healthcare. *npj Digit. Med.* 4, 45. doi:10.1038/s41746-021-00418-3

Soref, R., Peale, R. E., and Buchwald, W. (2008). Longwave plasmonics on doped silicon and silicides. *Opt. Express* 16, 6507–6514. doi:10.1364/oe.16.006507

Soref, R. (2006). The past, present, and future of silicon photonics. *IEEE J. Sel. Top. Quantum Electron.* 12, 1678–1687. doi:10.1109/JSTQE.2006.883151

Sreekanth, K. V., Alapan, Y., Elkabbash, M., Ilker, E., Hinczewski, M., Gurkan, U. A., et al. (2016). Extreme sensitivity biosensing platform based on hyperbolic metamaterials. *Nat. Mat.* 15, 621–627. doi:10.1038/nmat4609

Steinberger, B., Hohenau, A., Ditlbacher, H., Aussenegg, F. R., Leitner, A., and Krenn, J. R. (2007). Dielectric stripes on gold as surface plasmon waveguides: Bends and directional couplers. *Appl. Phys. Lett.* 91, 081111. doi:10.1063/1.2772774

Sterczewski, L. A., Bagheri, M., Frez, C., Canedy, C. L., Vurgaftman, I., and Meyer, J. R. (2020). Mid-infrared dual-comb spectroscopy with room-temperature bi-functional interband cascade lasers and detectors. *Appl. Phys. Lett.* 116, 141102. doi:10.1063/1.5143954

Strazdaite, S., Navakauskas, E., Kirschner, J., Sneideris, T., and Niaura, G. (2020). Structure determination of hen egg-white lysozyme aggregates adsorbed to lipid/water and air/water interfaces. *Langmuir* 36, 4766–4775. doi:10.1021/acs.langmuir.9b03826

Streyer, W., Law, S., Rosenberg, A., Roberts, C., Podolskiy, V. A., Hoffman, A. J., et al. (2014). Engineering absorption and blackbody radiation in the far-infrared with surface phonon polaritons on gallium phosphide. *Appl. Phys. Lett.* 104, 131105. doi:10.1063/1.4870255

Submarine Communication (2023). Worldwide submarine communication fibers map. Available at: https://www.submarinecablemap.com/.

Süess, M. J., Jouy, P., Bonzon, C., Wolf, J. M., Gini, E., Beck, M., et al. (2016). Single-mode quantum cascade laser array emitting from a single facet. *IEEE Photonics Technol. Lett.* 28, 1197–1200. doi:10.1109/LPT.2016.2533443

Suess, M. J., Peretti, R., Liang, Y., Wolf, J. M., Bonzon, C., Hinkov, B., et al. (2016). Advanced fabrication of single-mode and multi-wavelength MIR-QCLs. *Photonics* 3, 26–18. doi:10.3390/photonics3020026

Szedlak, R., Hayden, J., Martín-Mateos, P., Holzbauer, M., Harrer, A., Schwarz, B., et al. (2018). Surface emitting ring quantum cascade lasers for chemical sensing. *Opt. Eng.* 57, 1. doi:10.1117/1.OE.57.1.011005

Szwarcman, D., Penello, G. M., Kawabata, R. M., Pires, M. P., and Souza, P. L. (2021). Quantifying milk proteins using infrared photodetection for portable equipment. *J. Food Eng.* 308, 110676. doi:10.1016/j.jfoodeng.2021.110676

Taliercio, T., and Biagioni, P. (2019). Semiconductor infrared plasmonics. *Nanophotonics* 8, 949–990. doi:10.1515/nanoph-2019-0077

Thongrattanasiri, S., Adams, D. C., Wasserman, D., and Podolskiy, V. A. (2011). Multiscale beam evolution and shaping in corrugated plasmonic systems. *Opt. Express* 19, 9269. doi:10.1364/oe.19.009269

Tombez, L., Schilt, S., Di Francesco, J., Führer, T., Rein, B., Walther, T., et al. (2012). Linewidth of a quantum-cascade laser assessed from its frequency noise spectrum and impact of the current driver. *Appl. Phys. B Lasers Opt.* 109, 407–414. doi:10.1007/s00340-012-5005-x

Tuzson, B., Mangold, M., Looser, H., Manninen, A., and Emmenegger, L. (2013). Compact multipass optical cell for laser spectroscopy. *Opt. Lett.* 38, 257–259. doi:10.1364/OL.38.000257

Tuzson, B., Mohn, J., Zeeman, M. J., Werner, R. A., Eugster, W., Zahniser, M. S., et al. (2008). High precision and continuous field measurements of $\delta^{13}C$ and $\delta^{18}O$ in carbon dioxide with a cryogen-free QCLAS. *Appl. Phys. B Lasers Opt.* 92, 451–458. doi:10.1007/s00340-008-3085-4

Van Geldern, R., Nowak, M. E., Zimmer, M., Szizybalski, A., Myrttinen, A., Barth, J. A., et al. (2014). Field-based stable isotope analysis of carbon dioxide by mid-infrared laser spectroscopy for carbon capture and storage monitoring. *Anal. Chem.* 86, 12191–12198. doi:10.1021/ac5031732

Villares, G., Hugi, A., Blaser, S., and Faist, J. (2014). Dual-comb spectroscopy based on quantum-cascade-laser frequency combs. *Nat. Commun.* 5, 5192–5193. doi:10.1038/ncomms6192

Vurgaftman, I., Bewley, W. W., Canedy, C. L., Kim, C. S., Kim, M., Merritt, C. D., et al. (2013). Interband cascade lasers with low threshold powers and high output powers. *IEEE J. Sel. Top. Quantum Electron.* 19, 1200210. doi:10.1109/JSTQE.2012.2237017

Wacht, D., David, M., Hinkov, B., Detz, H., Schwaighofer, A., Baumgartner, B., et al. (2022). Mesoporous Zirconia coating for sensing applications using attenuated total reflection fourier transform infrared (ATR FT-IR) spectroscopy. *Appl. Spectrosc.* 76, 141–149. doi:10.1177/00037028211057156

Waclawek, J. P., Kristament, C., Moser, H., and Lendl, B. (2019). Balanced-detection interferometric cavity-assisted photothermal spectroscopy. *Opt. Express* 27, 12183–12195. doi:10.1364/OE.27.012183

Waclawek, J. P., Moser, H., and Lendl, B. (2016). Compact quantum cascade laser based quartz-enhanced photoacoustic spectroscopy sensor system for detection of carbon disulfide. *Opt. Express* 24, 6559. doi:10.1364/OE.24.006559

Wang, Z., Wang, Q., Ching, J. Y. L., Wu, J. C. Y., Zhang, G., and Ren, W. (2017). A portable low-power QEPAS-based CO2 isotope sensor using a fiber-coupled interband cascade laser. *Sensors Actuators, B* 246, 710–715. doi:10.1016/j.snb.2017.02.133

Wasserman, D., Shaner, E. A., and Cederberg, J. G. (2007). Midinfrared doping-tunable extraordinary transmission from sub-wavelength Gratings. *Appl. Phys. Lett.* 90, 191102. doi:10.1063/1.2737138

Weih, R., Nähle, L., Höfling, S., Koeth, J., and Kamp, M. (2014). Single mode interband cascade lasers based on lateral metal gratings. *Appl. Phys. Lett.* 105, 071111. doi:10.1063/1.4893788

Williams, C. R., Andrews, S. R., Maier, S. A., Fernández-Domínguez, A. I., Martín-Moreno, L., and García-Vidal, F. J. (2008). Highly confined guiding of terahertz surface plasmon polaritons on structured metal surfaces. *Nat. Photonics* 2, 175–179. doi:10.1038/nphoton.2007.301

Williams, S. M., and Coe, J. V. (2006). Dispersion study of the infrared transmission resonances of freestanding Ni microarrays. *Plasmonics* 1, 87–93. doi:10.1007/s11468-005-9001-4

Wu, C., Khanikaev, A. B., Adato, R., Arju, N., Yanik, A. A., Altug, H., et al. (2012). Fano-resonant asymmetric metamaterials for ultrasensitive spectroscopy and identification of molecular monolayers. *Nat. Mat.* 11, 69–75. doi:10.1038/nmat3161

Wu, H., Dong, L., Zheng, H., Yu, Y., Ma, W., Zhang, L., et al. (2017). Beat frequency quartz-enhanced photoacoustic spectroscopy for fast and calibration-free continuous trace-gas monitoring. *Nat. Commun.* 8, 15331. doi:10.1038/ncomms15331

Wunderlin, P., Lehmann, M. F., Siegrist, H., Tuzson, B., Joss, A., Emmenegger, L., et al. (2013). Isotope signatures of N_2O in a mixed microbial population system: Constraints on N_2O producing pathways in wastewater treatment. *Environ. Sci. Technol.* 47, 1339–1348. doi:10.1021/es303174x

Wysocki, G., Curl, R. F., Tittel, F. K., Maulini, R., Bulliard, J. M., and Faist, J. (2005). Widely tunable mode-hop free external cavity quantum cascade laser for high resolution spectroscopic applications. *Appl. Phys. B Lasers Opt.* 81, 769–777. doi:10.1007/s00340-005-1965-4

Xie, Q., Deng, S., Schaekers, M., Lin, D., Caymax, M., Delabie, A., et al. (2012). Germanium surface passivation and atomic layer deposition of high-k dielectrics - a tutorial review on Ge-based MOS capacitors. *Semicond. Sci. Technol.* 27, 074012. doi:10.1088/0268-1242/27/7/074012

Yang, H., Yang, S., Kong, J., Dong, A., and Yu, S. (2015). Obtaining information about protein secondary structures in aqueous solution using Fourier transform IR spectroscopy. *Nat. Protoc.* 10, 382–396. doi:10.1038/nprot.2015.024

Yang, R. Q. (1995). Infrared laser based on intersubband transitions in quantum wells. *Superlattices Microstruct.* 17, 77–83. doi:10.1006/spmi.1995.1017

Yang, R. Q., Tian, Z., Cai, Z., Klem, J. F., Johnson, M. B., and Liu, H. C. (2010). Interband-cascade infrared photodetectors with superlattice absorbers. *J. Appl. Phys.* 107, 054514. doi:10.1063/1.3327415

Yashunsky, V., Zilberstein, A., Marciano, T., Lirtsman, V., Golosovsky, M., Davidov, D., et al. (2010). Infrared surface plasmon spectroscopy of living cells. *AIP Conf. Proc.* 1281, 1617–1621. doi:10.1063/1.3498133

Yoo, D., Mohr, D. A., Vidal-Codina, F., John-Herpin, A., Jo, M., Kim, S., et al. (2018). High-contrast infrared absorption spectroscopy via mass-produced coaxial zero-mode resonators with sub-10 nm gaps. *Nano Lett.* 18, 1930–1936. doi:10.1021/acs.nanolett.7b05295

Yu, N., Fan, J., Wang, Q. J., Pflügl, C., Diehl, L., Edamura, T., et al. (2008). Small-divergence semiconductor lasers by plasmonic collimation. *Nat. Photonics* 2, 564–570. doi:10.1038/nphoton.2008.152

Yu, N., Wang, Q. J., Kats, M. A., Fan, J. A., Khanna, S. P., Li, L., et al. (2010). Designer spoof surface plasmon structures collimate terahertz laser beams. *Nat. Mat.* 9, 730–735. doi:10.1038/nmat2822

Zhang, B., Bian, Y., Ren, L., Guo, F., Tang, S. Y., Mao, Z., et al. (2017). Hybrid dielectric-loaded nanoridge plasmonic waveguide for low-loss light transmission at the subwavelength scale. *Sci. Rep.* 7, 40479–9. doi:10.1038/srep40479

Zhong, Y., Malagari, S. D., Hamilton, T., and Wasserman, D. (2015). Review of mid-infrared plasmonic materials. *J. Nanophot.* 9, 093791. doi:10.1117/1.jnp.9.093791

Glossary

ATR	attenuated total reflection
BI-CAPS	balanced detection cavity-assisted photothermal spectroscopy
BSA	bovine serum albumin
CW	continuous-wave
DFB	distributed feedback
DL	dielectric loading
EC	external-cavity
EOT	extraordinary optical transmission
FRAMM	Fano-resonant asymmetric metamaterial
FTIR	Fourier-transform infrared
ICIP	interband cascade infrared photodetector
ICL	interband cascade laser
IRAS	infrared reflection absorption spectroscopy
LED	light emitting diode
LSP	localized surface plasmon
MCT	mercury cadmium telluride
mid-IR	mid-infrared
near-IR	near-infrared
PIC	photonic integrated circuit
PLL	poly-l-lysine
PLS	partial least square
RT	room temperature
QCD	quantum cascade detector
QCL	quantum cascade laser
QEPAS	quartz-enhanced photoacoustic spectroscopy
SEIRA	surface-enhanced IR absorption spectroscopy
SERS	surface-enhanced Raman spectroscopy
SL	semiconductor loading
SPEIRA	surface-plasmon-enhanced IR absorption
SPP	surface plasmon polariton
SPR	surface-plasmon resonance
TM	transverse magnetic